control while avoiding the critical motor starting problem, associated line disturbance, and altitude brush problems of a servomotor control.

References

1. Report on Advisory Staff for Aircraft Electric Systems. Wright Air Development Center and Bureau of Aeronautics, Dayton, Ohio, 1951, pages 21, 45, 56.

2. Research and Development in the United States Air Force, **Major General Donald L. Putt.** *SAE Quarterly Transactions* (New York, N. Y.), volume 6, number 2, April 1952, pages 304–07.

3. Electronic Instruments (book), **J. A. Greenwood, Jr., J. V. Holdam, Jr., D. MacRae, Jr.** MIT Radiation Laboratory Series Number 21, McGraw-Hill Book Company, Inc., New York, N. Y., 1948, pages 386–436.

4. A Polarized Relay as an Aircraft Control Element, **Royce E. Johnson, Frank A. Glassow.** *AIEE Transactions*, volume 67, part II, 1948, pages 1249–55.

5. Sensitive Relay Contact Protection Systems, **J. P. Dallas, T. H. McCully.** *AIEE Transactions*, volume 67, part II, 1948, pages 1204–07.

6. Electrostatic Oscillation in Sensitive Contact Mechanisms, **Thomas R. Stuelpnagel.** *AIEE Transactions*, volume 71, part II, 1952 (January 1953 Section), pages 397-401.

7. One Type of Rotary Magnetic Clutch and Its Associated Brake Used on Aircraft Electric Motors, **Leo Andrews, Fred Shanely.** *Electrical Engineering*, volume 63, number 12, December 1944, pages 893–95.

8. Braking Device for 400-Cycle Motors, **L. A. Zahorsky.** *Electrical Engineering*, volume 71, number 6, June 1952, pages 506–11.

9. Electronic Auto-Pilot Circuits, **W. H. Gille, H. T. Sparrow.** *Electronics* (New York, N. Y.), volume 17, October 1944, page 110.

No Discussion

Impedance Data for 400-Cycle Aircraft Distribution Systems

D. W. EXNER
MEMBER AIEE

G. H. SINGER, JR.
ASSOCIATE MEMBER AIEE

Synopsis: This paper presents impedance data which the authors have compiled for use in designing and testing aircraft electric systems employing 3-phase 400-cycle auxiliary power. Tabulated herein are impedance data for a number of typical configurations employing multiple-wire feeders in 0.5-inch flat spacing and laced 3-phase groups. Sufficient background material and procedure are given to enable the reader to calculate additional data for configurations not actually tabulated.

The positive-sequence data were calculated directly from the geometry of the wire configurations. However, zero-sequence data are dependent upon the particular ground return circuit employed and, therefore, these data are the result of a theoretical calculation modified by an empirically determined skin correction term. The experimental work carried out to obtain these skin correction values is described.

By nature a data presentation such as this is incomplete and somewhat restricted in usefulness. However, it is hoped that those involved in analytical and experimental studies on 3-phase 400-cycle aircraft systems will expand these data to include any new configurations which may be used.

SINCE the advent of large military aircraft with their ever-increasing dependence on auxiliary power for control and tactical functions, there has been a steady increase to higher voltage electric systems. One currently used system employs 120/208-volt 3-phase 400-cycle Y-connected electric power and multiple-wire feeders containing fusible limiters. The problems of fault clearing and limiter co-ordination occurring during short-circuit faults involve the transient characteristics and the sequence impedances of the rotating machinery and the sequence impedances of the circuit elements comprising the distribution system. Similar to the case of industrial power distribution networks, these fault problems are best handled by application of the symmetrical component theory. This study was undertaken because the necessary impedance data were not available for applying symmetrical components to aircraft wire configurations. Reference 1 provides excellent background for the work described here, but it was felt that this material should be expanded to include multiple wires per phase. Also, the effects of ground path on zero-sequence impedance required more thorough investigation, using an actual or a simulated aircraft structure.

Nomenclature

a = radius of solid round conductor, inches
t = time, seconds
L = inductance, henrys
I = current, amperes
μ = permeability = 4×10^{-7} weber per meter per ampere-turn
ln = natural logarithm, base = ϵ = 2.718
log = common logarithms, base = 10
d_s = GMR = self-geometric mean radius of a solid round conductor or a stranded conductor, inches
d^*_s = GMR of a 3-phase group of conductors, inches
GMD = mutual geometric mean distance between conductors i and j, inches
D_{ij} = linear distance between conductors i and j, inches
D = spacing of 3-phase groups, inches
s = spacing of individual conductors in a flat 3-phase group, inches
h = mean height of configuration above skin, inches
R = resistance, ohms per 1,000 feet per phase
R_0 = zero-sequence resistance
R_{0c} = calculated value of zero-sequence resistance assuming perfect ground plane
R_s = skin correction term for zero-sequence resistance
X = reactance, ohms per 1,000 feet per phase
X_0 = zero-sequence reactance
X_{0c} = calculated value of zero-sequence reactance assuming perfect ground place
X_s = skin correction term for zero-sequence reactance
Z = impedance
A = equivalent distance to return circuit

Approach to the Problem

In compiling these data it was assumed that the configurations most likely to be used in 3-phase aircraft systems were laced and that they were 0.5-inch flat spaced groups, as shown in Figure 1. Since various systems are likely to employ from one to five wires per phase at distances from the skin of up to 5 inches, it was felt that data should be available to include all these cases.

To make clear the methods used in determining these data, the pertinent theoretical background should be reviewed briefly. Considering a solid round conductor, it is possible to write an expression for the inductance per unit length as follows

$$L=\frac{\mu}{2\pi}\left(\frac{1}{4}+\ln\frac{A}{a}\right) \qquad (1)$$

The first term gives the inductance due to

Paper 52-322, recommended by the AIEE Air Transportation Committee and approved by the AIEE Committee on Technical Operations for presentation at the AIEE Middle Eastern District Meeting, Toledo, Ohio, October 28–30, 1952. Manuscript submitted July 25, 1952; made available for printing October 6, 1952.

D. W. Exner and G. H. Singer, Jr., are with the Boeing Airplane Company, Seattle, Wash.

The work on which this paper is based was carried out by the Acoustics-Electrical Unit of the Boeing Airplane Company, Seattle, Wash.

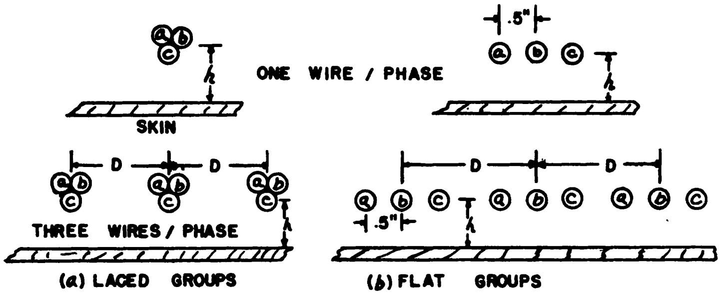

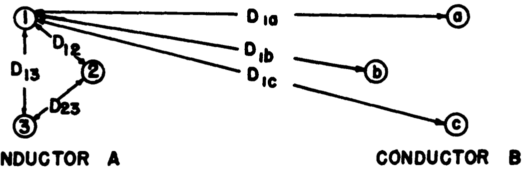

Figure 1 (left)

Figure 3 (above)

the internal flux linkages, and the second term the inductance due to the external linkages. A powerful tool in the calculation of the inductance of a configuration of conductors is the concept of a geometric mean distance. For example, equation 1 can be written

$$L=\frac{\mu}{2\pi}\ln\frac{A}{a\epsilon^{-0.25}}=\frac{\mu}{2\pi}\ln\frac{A}{d_s} \qquad (2)$$

This is equivalent to replacing the solid round conductor by a hollow tube having negligible internal inductance and a radius equal to $a\epsilon^{-0.25}$. This radius is called the self-geometric mean radius of a solid round conductor, abbreviated GMR, or d_s. Equation 2 is important in inductance calculations because it can be used for conductors of any shape or stranding provided the proper GMR is used. The calculation of GMR is merely a geometry problem and is considered in detail in reference 2.

Figure 2 shows a circuit consisting of two arbitrarily shaped current-carrying conductors A and B consisting of n and m individual parts respectively. The following expression for the inductance per unit length for conductor A is developed in reference 3.

$$L=\frac{\mu}{2\pi}\ln\frac{\text{GMD}}{\text{GMR}} \qquad (3)$$

where

$$\text{GMD}=(D_{a1}D_{b1}\ldots D_{a2}D_{b2}\ldots D_{an}D_{bn}\ldots)^{1/mn} \qquad (4)$$

$$\text{GMD}=(d_{s1}D_{12}D_{13}\ldots d_{s2}D_{21}D_{23}\ldots d_{sn}D_{n1}D_{n2}\ldots)^{1/n^2} \qquad (5)$$

The numerator of the logarithmic term is the mutual geometric mean spacing between the n elements of A and the m elements of B, abbreviated GMD. As seen from equation 4, the computation of GMD involves all the mutual spacings between the elements of the conductors A and B, and the GMR involves the geometric mean radii of all the components of A and the spacings between components. The following example illustrates the use of equations 3, 4, and 5 in computing inductance.

Consider the problem of determining the inductance of the single-phase transmission line whose geometry is given in Figure 3. Since the conductors are all similar, equation 5 for GMR reduces to

$$\text{GMR}=[d_s^{n/2}D_{12}\ldots D_{1n}\ \ D_{23}\ldots D_{2n}\ldots D_{(n-1)n}]^{2/n^2} \qquad (6)$$

Therefore, for Figure 3

$$\text{GMR}=[d_s^{3/2}D_{12}D_{23}D_{31}]^{2/9} \qquad (7)$$

Using equation 4, GMD becomes

$$\text{GMD}=[D_{1a}D_{1b}D_{1c}\ \ D_{2a}D_{2b}D_{2c}\ \ D_{3a}D_{3b}D_{3c}]^{1/9} \qquad (8)$$

Substituting equations 7 and 8 in equation 3, the inductance per unit length of the single-phase line of Figure 3 can be calculated if the physical spacing and geometric radii are known.

This method, outlined for a single-phase line, leads directly to the calculation of the zero-sequence impedance of aircraft transmission lines. In large military aircraft the electric power distribution circuits often run normal to the circumferential body stiffeners about 3 to 5 inches from the metal skin or along the main wing spars. Under ground-fault conditions the zero-sequence fault current is, by definition, the single-phase component flowing through the conductors of the faulted circuit into the fault and returning through the grounding system. Consider the line shown in Figure 4 (A) representing the zero-sequence path of an aircraft circuit. To calculate rigorously the impedance as seen from points 1 and 2 of this circuit, a knowledge of the current distribution in the ground plane must be available. Without an extensive mathematical analysis, which even then involves certain approximations, this distribution cannot be defined.

Because of the inability of solving the circuit of Figure 4(A) completely by theoretical methods, the following approach was used. First, the ground plane was considered to be a perfect ground return, and the impedance of the conductor configuration was calculated by image theory. Second, a correction term, determined empirically, was applied to the calculated value to account for the fact that the actual skin is not a perfect ground. A perfect ground plane is defined as a plane sheet of infinite extent having zero resistance and inductance. With such a return circuit, the distribution of the electric and magnetic fields above the ground plane is identical to that existing for a 2-sided line with a return circuit whose configuration is the image of the actual conductors and is located an equal distance below the position of the ground sheet. The image configuration for this line is shown in Figure 4 (B).

Measurements were carried out on 3-phase circuits set up in an *XC-97* air frame to determine the actual 400-cycle zero-sequence impedance for a number of typical configurations. These data then were compared with corresponding values calculated by image theory. Since it was impractical to obtain data for all possible

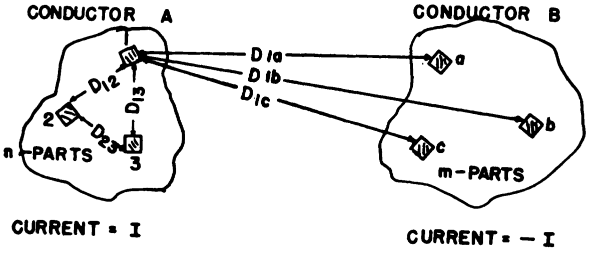

Figure 2

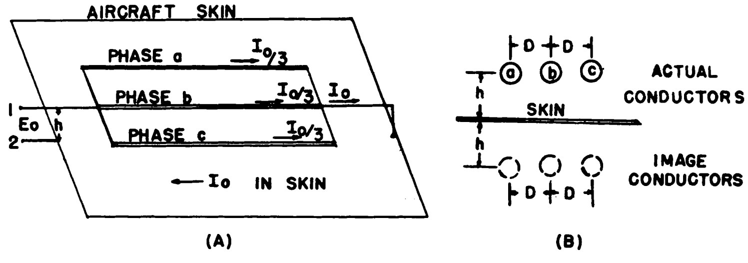

Figure 4

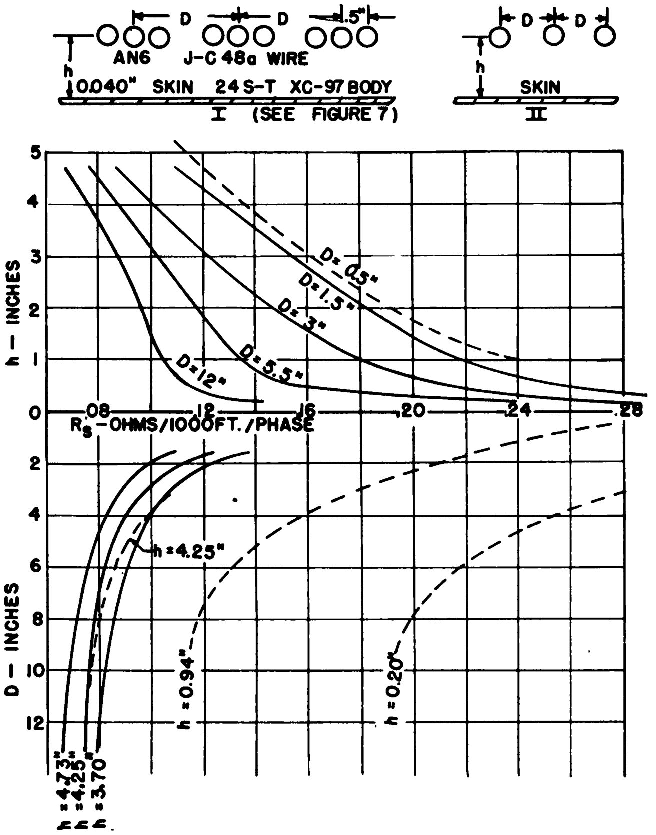

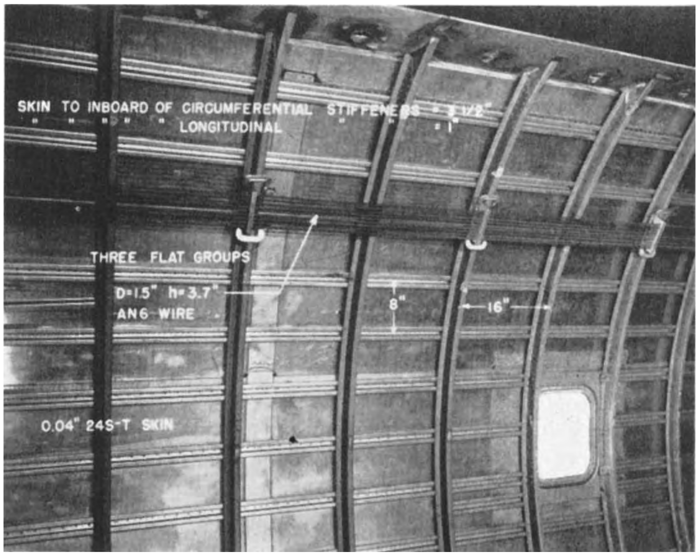

Figure 5 (left). Zero-sequence resistance correction terms from test at 400 cycles per second

Note: Solid curves are for configuration I. Broken curves are for configuration II. Actual test points were within 10 per cent of these curves

Figure 7 (above). Test air-frame structure

spacings and wire configurations, it was necessary to interpolate the data for those cases not actually tested. The skin correction terms are summarized in Figures 5 and 6; the *XC-97* structure is shown in Figure 7. Appendix I illustrates the development of the GMD and GMR equations for the configurations studied, and Appendix II gives the GMD and GMR equations. Appendix III gives examples of the calculation of the positive and zero-sequence data in Table II and in Figures 9 to 25. Appendix IV discusses the test work briefly.

Presentation of Data

The 400-cycle impedance data for aircraft wire configurations resulting from this study are summarized in Table II and in Figures 9 to 25. These data should be adequate for analytical and design work on electrical distribution systems for large aircraft. Only data for laced 3-phase groups and 3-phase groups in 0.5-inch flat spacing have been compiled, since these configurations were considered the most likely to be used in present designs. The following statements are made to clarify the use of Table II and Figures 9 to 25:

1. The positive-sequence impedance data are all calculated values based on *AN-J-C-48a* (Army-Navy) wire specifications and on the 400-cycle resistance information contained in reference 4. These data are not affected by the type of body structure or by whether or not the wires are run in nonmagnetic conduit. Also, the elevation of the configuration above the aircraft skin has no effect on the positive-sequence impedance.
2. The zero-sequence data were compiled by calculating the theoretical impedance assuming an infinite perfect skin return circuit and then applying empirical correction terms to account for the actual skin

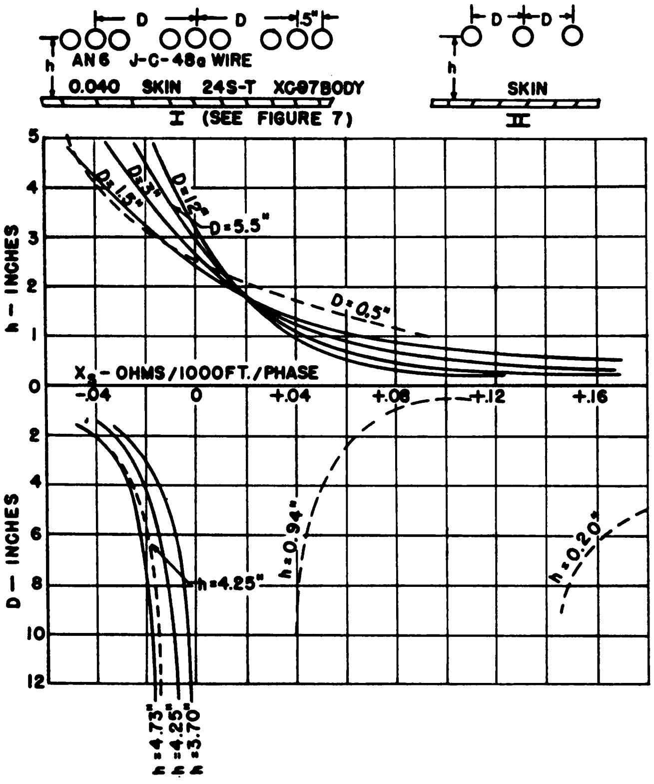

Figure 6 (left). Zero - sequence reactance correction terms from test at 400 cycles per second

Note: Solid curves are for configuration I. Broken curves are for configuration II. Actual test points were within 10 per cent of these curves

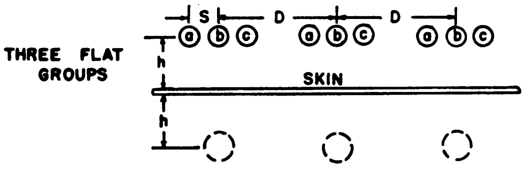

Figure 8 (right)

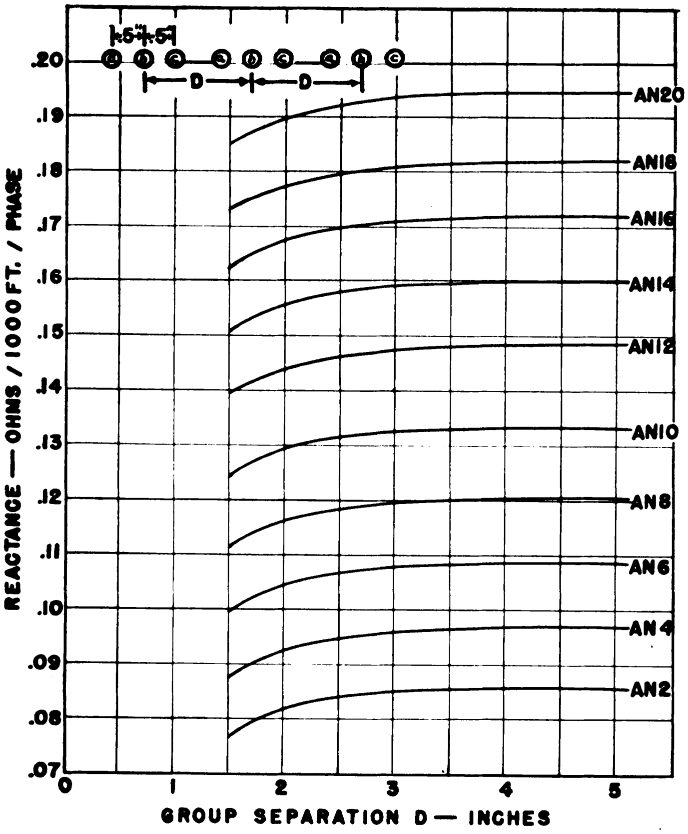

RESISTANCE — OHMS / 1000 FT. / PHASE									
AN20	AN18	AN16	AN14	AN12	AN10	A.N8	AN6	AN4	AN2
3.42	2.15	1.59	.997	.627	.366	.234	.147	.094	.063

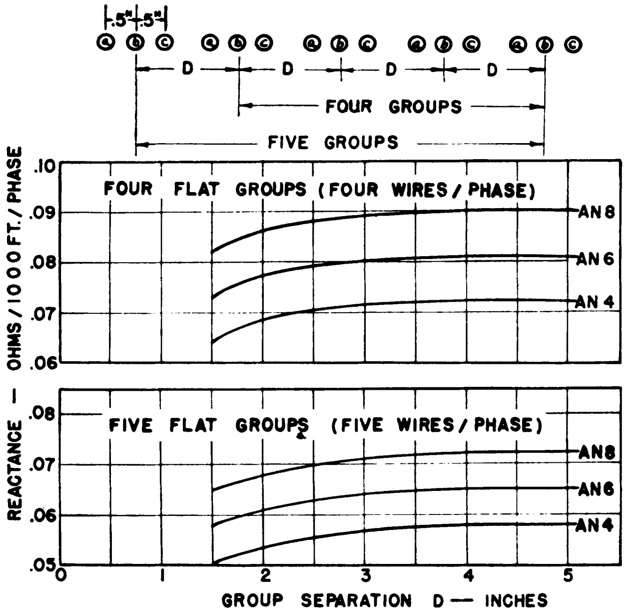

	RESISTANCE — OHMS / 1000 FT. / PHASE									
	AN20	AN18	AN16	AN14	AN12	AN10	AN8	AN 6	AN 4	AN 2
FOUR FLAT GROUPS	2.55	1.61	1.19	.747	.470	.275	.175	.110	.071	.047
FIVE FLAT GROUPS	2.05	1.29	.952	.598	.376	.220	.140	.088	.056	.038

Figure 9 (left). Positive-sequence impedance for three flat groups at 400 cycles per second

Figure 10 (above). Positive-sequence impedance for four and five flat groups at 400 cycles per second

structure. These correction terms were determined for a body structure which is considered typical of modern large aircraft designs. Due to the relatively small magnitude of this skin correction term for most wire configurations, and the impracticability of determining it exactly for all variations of body structure, the zero-sequence data presented in the following may be used without qualification.

3. The zero-sequence reactance is read directly from the curves for the proper size, elevation, and group separation. However, the zero-sequence resistance is obtained by adding the value R_{0c} from the table in each figure to the value of R_s from the R_s curve for the proper group separation. R_{0c} is the calculated zero-sequence resistance, assuming a perfect ground return, and R_s is the skin correction term.

4. The positive- and zero-sequence data for configurations employing four and five 3-phase groups were compiled for *AN-8*, *AN-6*, and *AN-4* wire sizes only, since these sizes are most likely to be used whenever the load requirements necessitate the use of four or five wires per phase.

5. Experimentation has shown that the zero-sequence impedance of wires run in grounded conduit is considerably different from the impedance when no conduit is used. At the time of this study, it was not possible to consider the effect of grounded conduit thoroughly. However, since the use of conduit probably will be held to a minimum in aircraft, due to weight considerations, it is felt that the conduit data summarized in Appendix V and Figure 25 are adequate. The positive-sequence impedance is not affected by the presence of nonmagnetic conduit.

6. All resistance data are computed at 20 degrees centigrade.

Appendix I. Development of GMD and GMR Equations

Zero-Sequence Equations

Example 1: Determine GMD and GMR for the 3-wire circuit of Figure 4(B). Using equation 4 the GMD between the three conductors and the image circuit is

$$\mathrm{GMD}=[(2h)^3(4h^2+D^2)^2(4h^2+4D^2)]^{1/9} \quad (9)$$

From equation 6 the GMR for the circuit of Figure 4(B) can be expressed

$$\mathrm{GMR}=(d_s^{3/2}D2DD)^{2/9}=1.166d_s^{1/3}D^{2/3} \quad (10)$$

Example 2: Determine GMD and GMR for the three 3-phase groups shown in Figure 8. The expression for the GMD is identical to equation 9, since each group can be considered as a single equivalent conductor for purposes of calculating the mutual spacing between the actual and image conductors.

In calculating the GMR of the actual conductor configuration, it is also possible to consider each 3-phase group as a single equivalent conductor whenever the spacings between the conductors of a group are small compared to the separation of the groups. It has been determined that this approach is valid for all spacings of laced groups and for groups in 0.5-inch flat spacing whenever the group spacing D is at least 3 inches. Therefore, for Figure 8

$$\mathrm{GMR}=1.166d^*{}_s{}^{1/3}D^{2/3} \quad \begin{cases}\text{laced groups: all values } D\\ \text{flat groups: } D>3 \text{ inches}\end{cases} \quad (11)$$

where $d^*{}_s$ is the GMR of a single group, expressed as

$$d^*{}_s=(d_s^{3/2}D_{ab}D_{bc}D_{ca})^{2/9}$$

For flat groups where D is less than 3 inches equation 12 for GMR is developed, using equation 6 and considering all nine conductors of the configuration shown in Figure 8

$$\mathrm{GMR}=[d_s^{9/2}2^8s^9D^9(D^2-s^2)^6(D^2-4s^2)^2\times(4D^2-s^2)^2]^{2/81} \quad (12)$$

Equation 12 reduces as follows for 0.5-inch flat groups.

$$\begin{aligned} D&=1.5 \text{ inches:} & \mathrm{GMR}&=1.32d_s^{1/9}\\ D&=2 \text{ inches:} & \mathrm{GMR}&=1.63d_s^{1/9} \qquad (13)\\ D&\geq 3 \text{ inches:} & \mathrm{GMR}&=1.166d_s^{*1/3}D^{2/3}\end{aligned}$$

Positive-sequence Equations

For positive-sequence inductance equation 14 can be developed for transposed 3-phase systems[3]

$$L=\frac{\mu}{2\pi}\ln\frac{(D_{mab}D_{mbc}D_{mca})^{1/3}}{\mathrm{GMR}}=\frac{\mu}{2\pi}\ln\frac{\mathrm{GMD}}{\mathrm{GMR}} \quad (14)$$

Table I. AN-J-C-48a Wire Data

Cable Size	D-C Resistance (Maximum AN-J-C-48a), Ohms per 1,000 Feet at 20 Deg. Cent.	400-Cycle Resistance, Ohms per 1,000 Feet at 20 Deg. Cent. (per reference 4)	Continuous Loading, Amperes (AN-W-14a Amendment 2)		Weight (Approx. AN-J-C-48a) Pounds per Foot	Nominal Conductor Area, Circular Mils	Number of Wires, Minimum	Maximum Diameter of Stranded Conductor, Inches	Diameter of Finished Cable, Inches	Self-GMR		
			Single Wire in Air	In Bundles						Single Wire d_s	3-Phase Group Laced d^*_s	3-Phase Group 1/2-Inch Flat d^*_s
AN-20	10.25	10.25	11	7.5	0.006	1,119	7	0.040	0.100	0.0138	0.0517	0.176
AN-18	6.44	6.44	16	10	0.009	1,779	7	0.050	0.115	0.0174	0.0613	0.190
AN-16	4.76	4.76	22	13	0.012	2,409	19	0.061	0.130	0.0213	0.0711	0.203
AN-14	2.99	2.99	32	17	0.018	3,830	19	0.076	0.150	0.0268	0.0845	0.219
AN-12	1.88	1.88	41	23	0.027	6,088	19	0.096	0.170	0.0338	0.0992	0.238
AN-10	1.10	1.10	55	33	0.043	10,443	37	0.122	0.200	0.0452	0.122	0.261
AN- 8	0.70	0.70	73	46	0.067	16,864	133	0.167	0.255	0.0582	0.156	0.284
AN- 6	0.436	0.440	101	60	0.100	26,813	133	0.218	0.310	0.0734	0.192	0.307
AN- 4	0.274	0.282	135	80	0.155	42,613	133	0.272	0.370	0.0925	0.233	0.332
AN- 2	0.179	0.188	181	100	0.250	66,832	663	0.345	0.445	0.1159	0.284	0.358
AN- 0	0.114	0.127	245	150	0.385	104,118	1,033	0.432	0.550	0.1450	0.353	

Table II. Positive-Sequence Impedance Data

(Three-Phase Groups, Ohms per 1,000 Feet per Phase at 400 Cycles per Second)

	One Flat Group 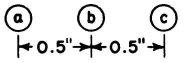	One Laced Group 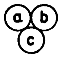	Three Laced Groups (3 Wires per Phase) 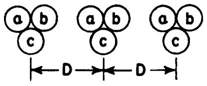	Four Laced Groups (4 Wires per Phase)	Five Laced Groups (5 Wires per Phase)
AN-20	10.25 +j0.585	10.25 +j0.304	3.42 +j0.101	2.56 +j0.076	2.05 +j0.061
AN-18	6.44 +j0.550	6.44 +j0.289	2.15 +j0.096	1.61 +j0.072	1.29 +j0.058
AN-16	4.76 +j0.519	4.76 +j0.278	1.59 +j0.093	1.19 +j0.070	0.952+j0.056
AN-14	2.99 +j0.484	2.99 +j0.264	0.997+j0.088	0.747+j0.066	0.598+j0.053
AN-12	1.88 +j0.448	1.88 +j0.247	0.627+j0.082	0.470+j0.062	0.376+j0.049
AN-10	1.10 +j0.405	1.10 +j0.228	0.366+j0.076	0.275+j0.057	0.220+j0.046
AN- 8	0.700+j0.366	0.700+j0.226	0.234+j0.075	0.175+j0.057	0.140+j0.045
AN- 6	0.440+j0.329	0.440+j0.221	0.147+j0.074	0.110+j0.055	0.088+j0.044
AN- 4	0.282+j0.294	0.282+j0.212	0.094+j0.071	0.071+j0.053	0.056+j0.042
AN- 2	0.188+j0.260	0.188+j0.206	0.063+j0.069	0.047+j0.052	0.038+j0.041
AN- 0		0.127+j0.204	0.042+j0.068	0.032+j0.051	0.025+j0.041

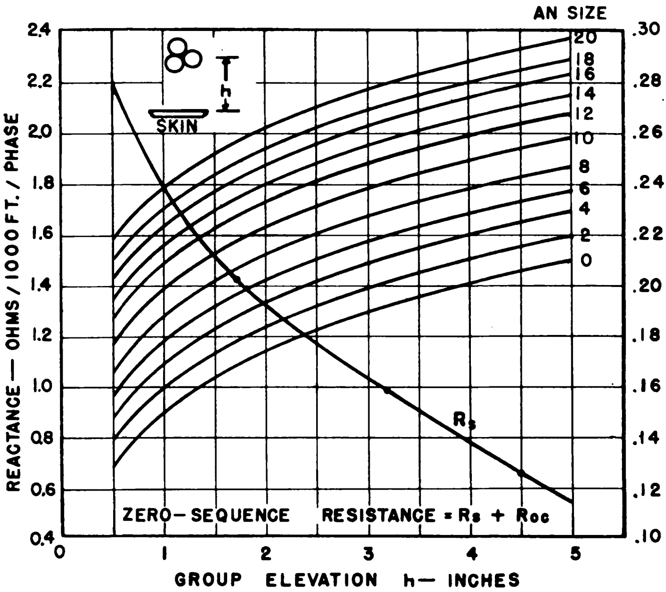

Roc — OHMS/ 1000 FT. / PHASE										
AN 20	AN 18	AN 16	AN 14	AN 12	AN 10	AN 8	AN 6	AN 4	AN 2	AN 0
10.25	6.44	4.76	2.99	1.88	1.10	.700	.440	.282	.188	.127

Figure 11. Zero-sequence impedance for one laced group at 400 cycles per second

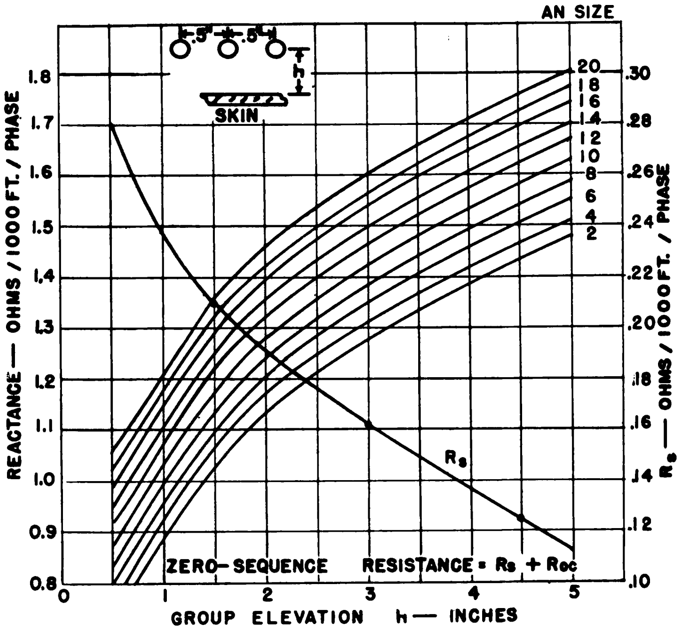

Roc — OHMS / 1000 FT. / PHASE										
AN 20	AN 18	AN 16	AN 14	AN 12	AN 10	AN 8	AN 6	AN 4	AN 2	AN 0
10.25	6.44	4.76	2.99	1.88	1.10	.700	.440	.282	.188	—

Figure 12. Zero-sequence impedance for one flat group at 400 cycles per second

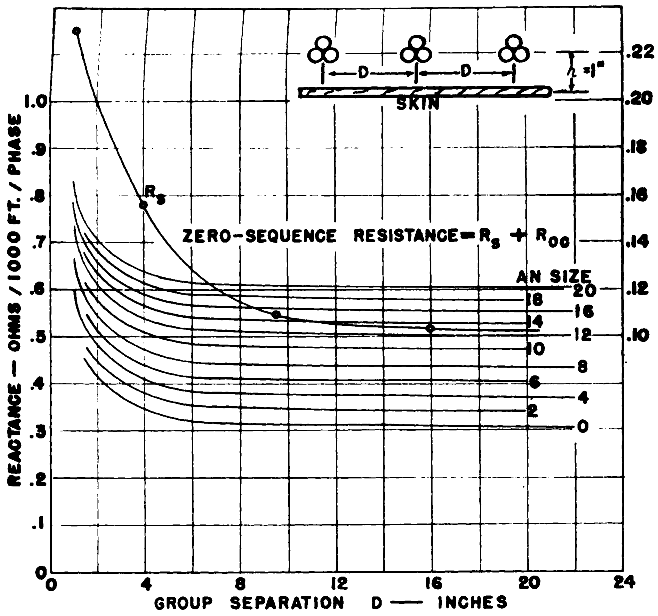

R0C — OHMS / 1000 FT. / PHASE										
AN20	AN18	AN16	AN14	AN12	AN10	AN 8	AN 6	AN 4	AN 2	AN 0
3.42	2.15	1.59	.997	.627	.366	.234	.147	.094	.063	.042

Figure 13. Zero-sequence impedance for three laced groups 1 inch above skin at 400 cycles per second

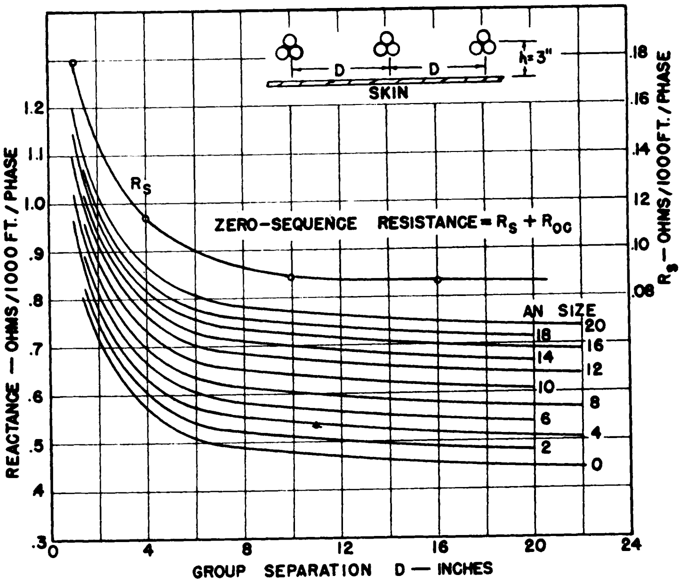

R0C — OHMS / 1000 FT. / PHASE										
AN20	AN18	AN16	AN14	AN12	AN10	AN 8	AN 6	AN 4	AN 2	AN 0
3.42	2.15	1.59	.997	.627	.366	.234	.147	.094	.063	.042

Figure 15. Zero-sequence impedance for three laced groups 3 inches above skin at 400 cycles per second

where D_{mab}, D_{mbc}, and D_{mca} are the GMD's between the respective phases as indicated by the subscripts, and the denominator is the GMR of one phase configuration. The computation of GMD and GMR for use in equation 14 as follows.

Example 3: Determine GMD and GMR for calculating the positive-sequence inductance of the circuit illustrated in Figure 8. Using equations 14 and 4 the GMD becomes

$$\text{GMD}=\left[\begin{array}{l} [s(D+s)(2D+s)(D-s)s\times \\ \qquad (D+s)(2D-s)(D-s)s]^{1/9} \\ [s(D+s)(2D+s)(D-s)s\times \\ \qquad (D+s)(2D-s)(D-s)s]^{1/9} \\ [2s(D-2s)(2D-2s)(D+2s)\times \\ \quad 2s(D-2s)(2D+2s)(D+2s)2s]^{1/9} \end{array}\right]^{1/3}$$
$$=[2^5s^9(D^2-s^2)^5(4D^2-s^2)^2\times (D^2-4s^2)^2]^{1/27} \quad (15)$$

By considering the three conductors of one phase and using equation 6, the GMR of a phase is

$$\text{GMD}=(d_s^{3/2}D2DD)^{2/9}=1.166d_s^{1/3}D^{2/3} \quad (16)$$

The positive-sequence inductance of configurations employing laced groups does not depend on the group separation, even for the closet spacings. Therefore, the per-phase impedance of a system employing n wires per phase is found by dividing the per-phase impedance of one laced group by n. This

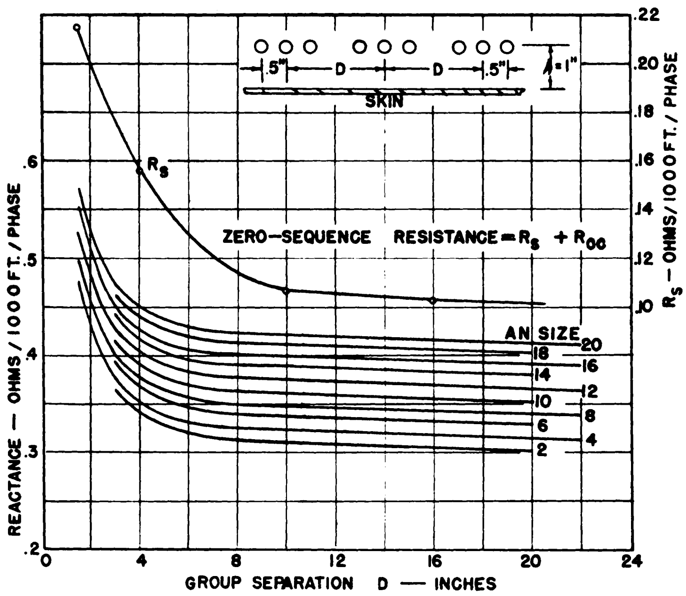

R0C — OHMS / 1000 FT. / PHASE										
AN20	AN18	AN16	AN14	AN12	AN10	AN 8	AN 6	AN 4	AN 2	AN0
3.42	2.15	1.59	.997	.627	.366	.234	.147	.094	.063	—

Figure 14. Zero-sequence impedance for three flat groups 1 inch above skin at 400 cycles per second

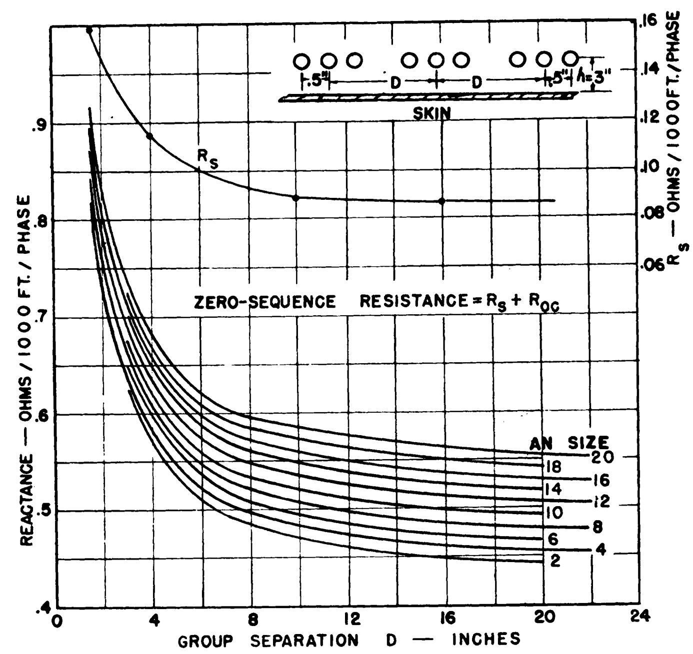

R0C — OHMS / 1000 FT. / PHASE										
AN20	AN18	AN16	AN14	AN12	AN10	AN 8	AN 6	AN 4	AN 2	AN 0
3.42	2.15	1.59	.997	.627	.366	.234	.147	.094	.063	—

Figure 16. Zero-sequence impedance for three flat groups 3 inches above skin at 400 cycles per second

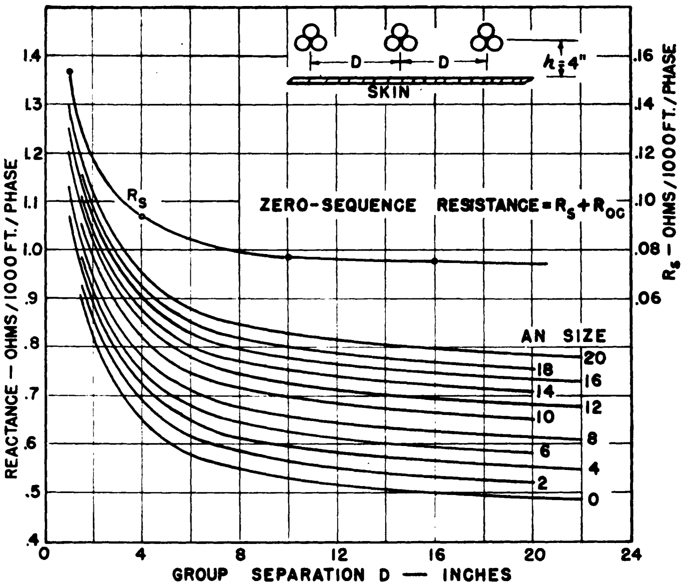

R_{OC} — OHMS / 1000 FT. / PHASE										
AN20	AN18	AN16	AN14	AN12	AN10	AN 8	AN 6	AN 4	AN 2	AN 0
3.42	2.15	1.59	.997	.627	.366	.234	.147	.094	.063	.042

Figure 17 (above). Zero-sequence impedance for three laced groups 4 inches above skin at 400 cycles per second

Figure 18 (right). Zero-sequence impedance for three flat groups 4 inches above skin at 400 cycles per second

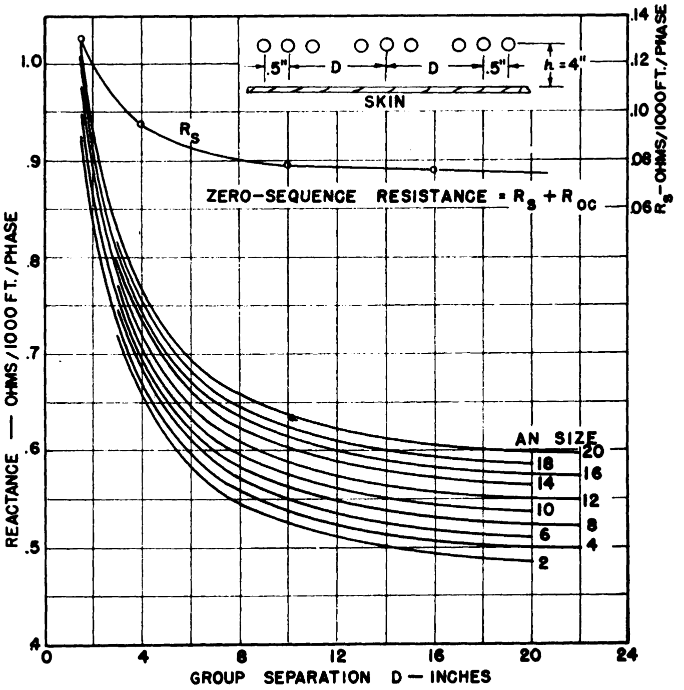

R_{OC} — OHMS / 1000 FT. / PHASE										
AN20	AN18	AN16	AN14	AN12	AN10	AN 8	AN 6	AN 4	AN 2	AN0
3.42	2.15	1.59	.997	.627	.366	.234	.147	.094	.063	——

is also true for groups in 0.5-inch flat spacing where the group separation exceeds about 5 inches (see Figures 9 and 10).

Equations for configurations of four and five 3-phase groups can be developed by the same procedure. Appendix II summarizes the equations developed for GMD and GMR of the configurations considered in this study.

Appendix II. GMD and GMR Equations

Positive-Sequence Equations

Three flat groups:

$$\mathrm{GMD} = [2^5 s^9 (D^2 - s^2)^5 (4D^2 - s^2)^2 \times (D^2 - 4s^2)^2]^{1/27}$$

$$\mathrm{GMR} = 1.166 d_s{}^{1/3} D^{2/3}$$

Four flat groups:

$$\mathrm{GMD} = [2^8 s^{12} (D^2 - s^2)^8 (4D^2 - s^2)^4 (D^2 - 4s^2)^3 \times (9D^2 - s^2)^2 (9D^2 - 4s^2)^2]^{1/48}$$

$$\mathrm{GMR} = (3.465 d_s D^3)^{1/4}$$

Five flat groups:

$$\mathrm{GMD} = [2^{13} s^{15} (D^2 - s^2)^{11} (D^2 - 4s^2)^4 \times (4D^2 - s^2)^7 (9D^2 - s^2)^4 \times (9D^2 - 4s^2)^2 (16D^2 - s^2)^2]^{1/75}$$

$$\mathrm{GMR} = (9.64 d_s D^4)^{1/5}$$

Zero-Sequence Equations

Three groups (laced or flat):

$$\mathrm{GMD} = [(2h)^3 (4h^2 + D^2)^2 (4h^2 + 4D^2)]^{1/9}$$

$$\text{(Laced): } \mathrm{GMR} = 1.166 d^*{}_s{}^{1/3} D^{2/3}$$

$$\text{(Flat)} \leftarrow \left[\begin{array}{ll} \mathrm{GMR} = 1.32 d_s{}^{1/9} & (D = 1.5'') \\ \mathrm{GMR} = 1.63 d_s{}^{1/9} & (D = 2'') \\ \mathrm{GMR} = 1.166 d^*{}_s{}^{1/3} D^{2/3} & (D \geq 3'') \end{array}\right.$$

Four groups (laced or flat):

$$\mathrm{GMD} = [(2h)^4 (4h^2 + D^2)^3 (4h^2 + 4D^2)^2 \times (4h^2 + 9D^2)]^{1/16}$$

$$\text{(Laced): } \mathrm{GMR} = (3.465 d^*{}_s D^3)^{1/4}$$

$$\text{(Flat)} \leftarrow \left[\begin{array}{ll} \mathrm{GMR} = 1.66 d_s{}^{1/12} & (D = 1.5'') \\ \mathrm{GMR} = 2.10 d_s{}^{1/12} & (D = 2'') \\ \mathrm{GMR} = (3.465 d^*{}_s D^3)^{1/4} & (D \geq 3'') \end{array}\right.$$

Five groups (laced or flat):

$$\mathrm{GMD} = [(2h)^5 (4h^2 + D^2)^4 (4h^2 + 4D^2)^3 \times (4h^2 + 9D^2)^2 (4h^2 + 16D^2)]^{1/25}$$

$$\text{(Laced): } \mathrm{GMR} = (9.64 d^*{}_s D^4)^{1/5}$$

$$\text{(Flat)} \leftarrow \left[\begin{array}{ll} \mathrm{GMR} = 1.97 d_s{}^{1/16} & (D = 1.5'') \\ \mathrm{GMR} = 2.53 d_s{}^{1/16} & (D = 2'') \\ \mathrm{GMR} = (9.64 d^*{}_s D^4)^{1/5} & (D \geq 3'') \end{array}\right.$$

Appendix III. Calculation of Impedance Data

To illustrate the general procedure followed in compiling the data presented in Table II and Figures 9 to 25, several sample calculations will be explained. It is felt that these examples, along with the preceding

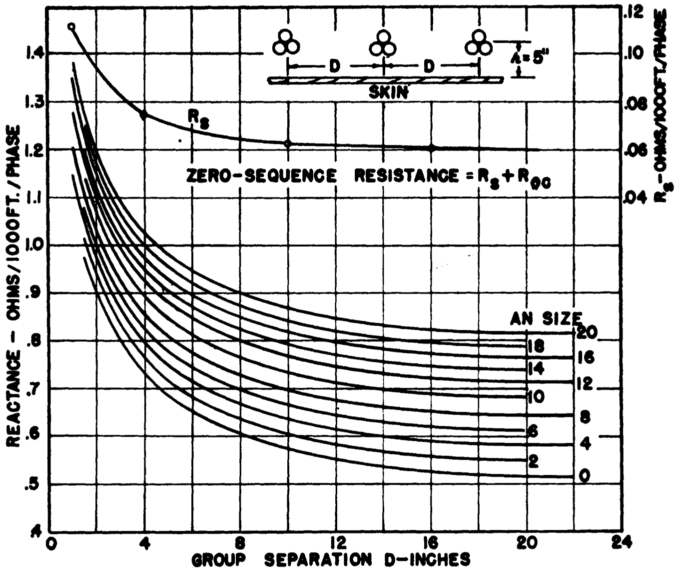

R_{OC} — OHMS / 1000 FT. / PHASE										
AN20	AN18	AN16	AN14	AN12	AN10	AN 8	AN6	AN 4	AN 2	AN0
3.42	2.15	1.59	.997	.627	.366	.234	.147	.094	.063	.042

Figure 19. Zero-sequence impedance for three laced groups 5 inches above skin at 400 cycles per second

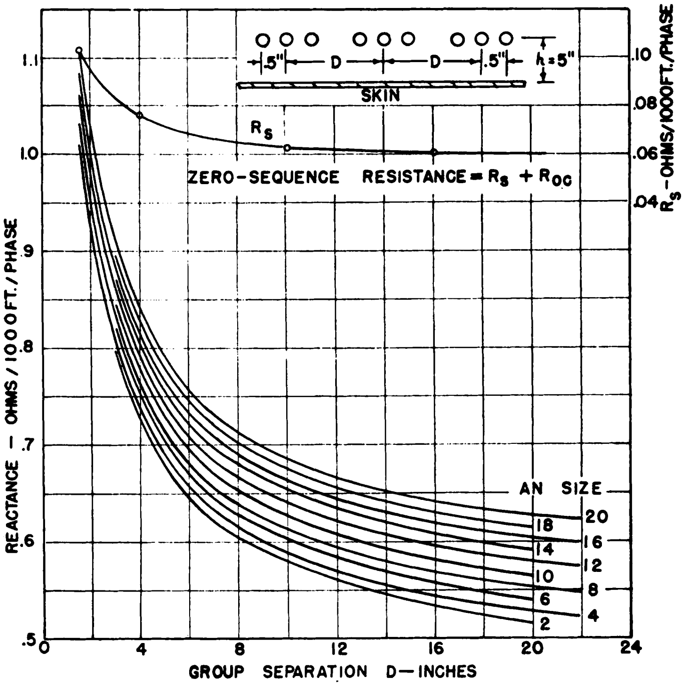

R_{OC} — OHMS/1000 FT./PHASE										
AN20	AN18	AN16	AN14	AN12	AN10	AN8	AN6	AN4	AN2	AN0
3.42	2.15	1.59	.997	.627	.366	.234	.147	.094	.063	—

Figure 20. Zero-sequence impedance for three flat groups 5 inches above skin at 400 cycles per second

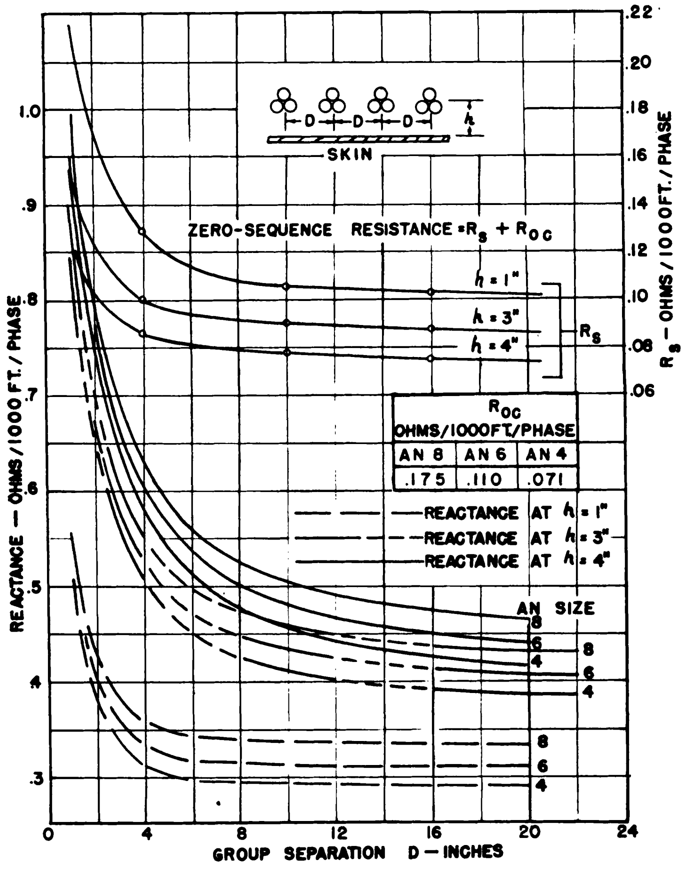

Figure 21. Zero-sequence impedance for four laced groups at 400 cycles per second

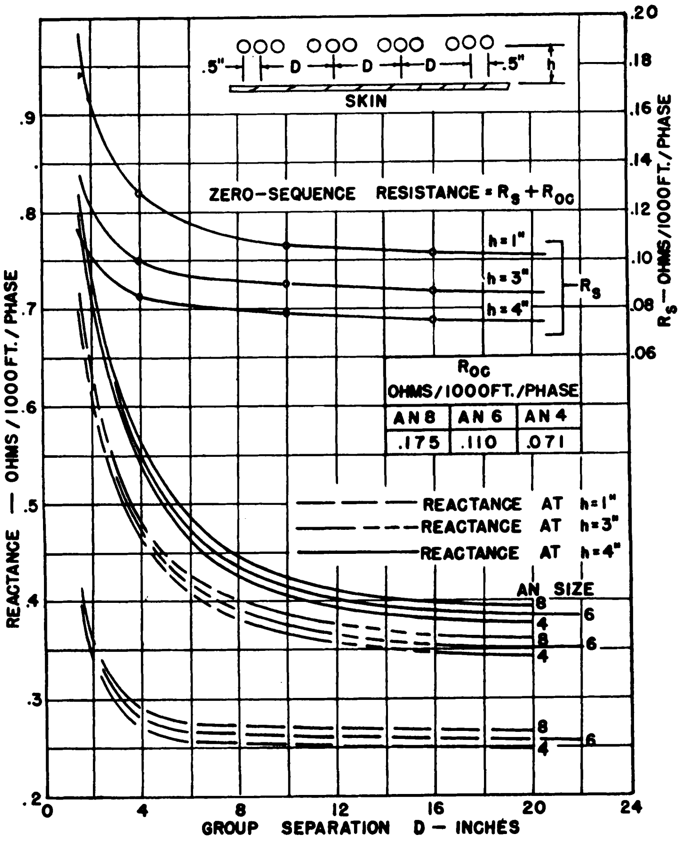

Figure 22. Zero-sequence impedance for four flat groups at 400 cycles per second

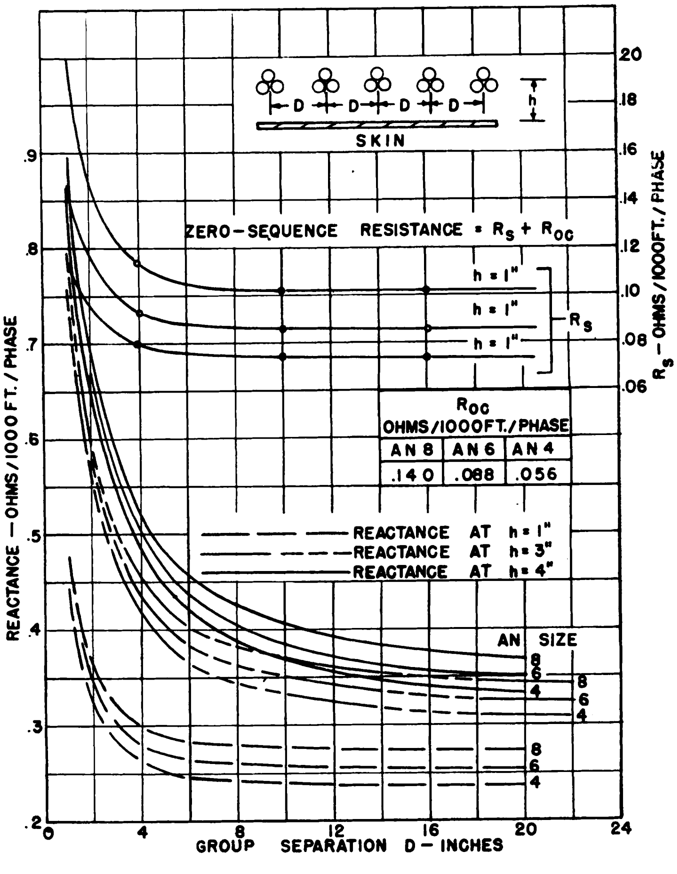

Figure 23. Zero-sequence impedance for five laced groups at 400 cycles per second

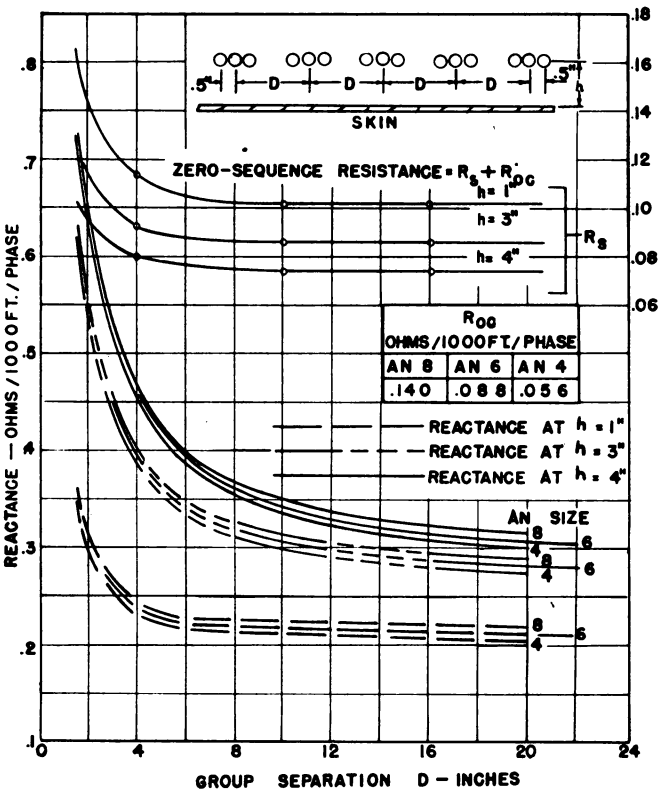

Figure 24. Zero-sequence impedance for five flat groups at 400 cycles per second

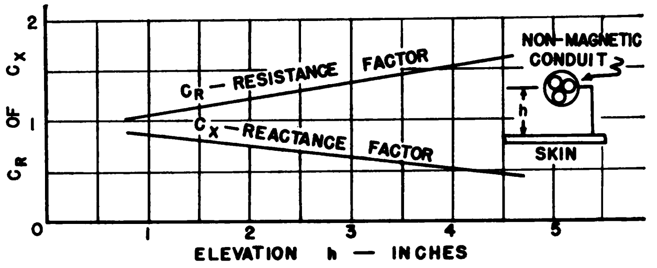

Figure 25. Zero-sequence impedance for laced groups in grounded conduit

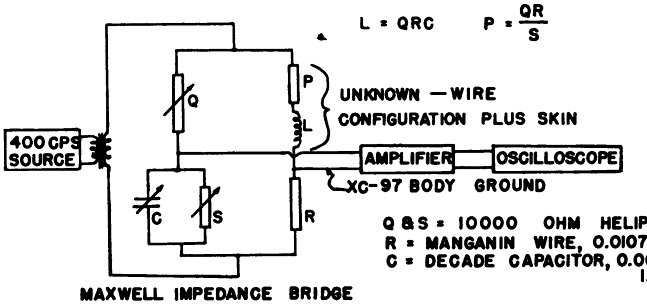

Figure 26. Bridge circuit used for impedance measurements

general material, will enable the user of the data to compile additional impedance information as the need arises.

Consider a 3-phase 400-cycle wire configuration consisting of three groups in 0.5-inch flat spacing (three wires per phase) having a group spacing D equal to 4 inches and an elevation h equal to 4 inches; see Figure 1(B). Assuming a wire size of *AN-6*, let it be required to find the positive- and zero-sequence impedance per 1,000 feet of this system of conductors. From the foregoing discussions, it is clear that the inductance can be determined in both cases by using the equation involving geometric mean distances, namely

$$L=\frac{\mu}{2\pi}\ln\frac{\text{GMD}}{\text{GMR}}\text{ henrys per meter} \qquad (17)$$

It is desirable to convert this equation to reactance at 400 cycles per second and also to use common instead of natural logarithms. The equation for 400-cycle reactance per 1,000 feet becomes

$$X=0.353\log_{10}\frac{\text{GMD}}{\text{GMR}}\text{ ohms per 1,000 feet} \qquad (18)$$

The equations for GMD and GMR of three flat groups from Appendix II are

$$\text{Positive sequence}\begin{cases}\text{GMD}=[2^5s^9(D^2-s^2)^5\times \\ \qquad (4D^2-s^2)^2(D^2-4s^2)^2]^{1/27} \\ \text{GMR}=1.166d_s{}^{1/3}D^{2/3}\end{cases} \qquad (19)$$

$$\text{Zero sequence}\begin{cases}\text{GMD}=[(2h)^3(4h^2+D^2)^2\times \\ \qquad (4h^2+4D^2)]^{1/9} \\ \text{GMR}=[1.166d^*{}_s{}^{1/3}D^{2/3}]\end{cases} \qquad (19A)$$

Data

$s=0.5$ inch
$D=4$ inches
$h=4$ inches
$d_s=$ GMR of single *AN-6* wire
$=0.0734$ inch (see Table I)
$d^*{}_s=$ GMR of 3-phase group
$=0.307$ inch (see Table I)

Calculations Using Equations 19 and (19A)

Positive sequence:
GMD = 2.50 inches
GMR = 1.232 inches

Zero sequence:
GMD = 9.10 inches
GMR = 1.972 inches

Therefore, from equation 18 the positive-sequence reactance is (all impedances are calculated in ohms per 1,000 feet per phase)

$$X_1=0.353\log_{10}\frac{2.50}{1.23}=0.1085 \qquad (20)$$

which checks the value in Figure 9.

With regard to the zero-sequence reactance of the configuration under discussion, equation 18 cannot be used directly. Even when assuming a perfect ground plane and, hence, no skin correction term, the value obtained from equation 18 gives the total reactance of the configuration of conductors above the skin. This value must be multiplied by 3 to obtain the zero-sequence reactance per phase. Using the values of GMD and GMR just given, the calculated (image) zero-sequence impedance becomes

$$X_{0c}=1.059\log_{10}\frac{9.10}{1.97}=0.704 \qquad (21)$$

The value of the skin correction term X_s can be found by interpolating the lower curves of Figure 6 for h equal to 4 inches. The value of zero-sequence reactance then becomes

$$X_0=X_{0c}+X_s=0.704-0.019=0.685 \qquad (22)$$

This value checks the corresponding point in Figure 18.

The positive-sequence resistance is found by dividing the value obtained for *AN-6* wire in Table I by 3. Hence

$$R_1=\frac{0.440}{3}=0.147 \qquad (23)$$

The calculated (image) value of zero-sequence resistance, assuming a perfect ground plane, is found by finding the parallel resistance of the conductor configuration above the skin and then multiplying by 3 to obtain the per-phase value. Hence

$$R_{0c}=\frac{0.440}{9}(3)=0.147 \qquad (24)$$

The value of the skin correction term R_s is found by interpolating the lower curves of Figure 5 for h equal to 4 inches. The value of zero-sequence resistance becomes

$$R_0=R_{0c}+R_s=0.147+0.095=0.242 \qquad (25)$$

Resistance values such as the foregoing can be obtained directly from Table II and Figures 9 to 25 according to the directions given in the section entitled "Presentation of Data."

Appendix IV. Test Work

The test work was carried out in an *XC-97* body having a skin of *24ST* alloy with an average thickness of 0.04 inch.

This structure (see Figure 7) was considered to be ideal for the test, since the size and distribution of the stiffening members and the general body design are representative of the large aircraft being engineered at the present time.

Three flat groups are shown arranged at a group separation of 1.5 inches and at an elevation of 4.7 inches above the skin. The nine wires are solidly connected together at each end of a 40-foot run, and the far end is grounded to the aircraft skin to simulate the zero-sequence circuit. Each configuration tested was arranged in this manner and then the circuit, consisting of the wires plus the skin return, was connected to an impedance bridge through calibrated leads. Theoretical considerations indicate that the size of wires, within the range normally encountered in aircraft installations, should not have an appreciable effect on the value of the skin correction terms. After several check tests to substantiate this hypothesis, *AN-6* wire was used throughout the tests involving the determination of skin correction terms.

With about 40 feet of clear wire run available in the *XC-97* body, a bridge circuit was required which would measure inductances accurately ranging from 1 to 20 microhenrys and resistance from 0.002 to 0.01 ohm. This represents approximately the values encountered in testing a single wire, three wires, and three 3-phase groups (nine wires). The Maxwell bridge circuit, described in Figure 26, was found to be very satisfactory for these measurements.

Appendix V. Zero-Sequence Impedance for Laced 3-Phase Groups in Grounded Conduit

Refer to Figure 25.

1. The zero-sequence impedance is not a function of the group spacing.

2. The zero-sequence impedance for one laced group in grounded solid-type conduit is found by multiplying the value found in Figure 7 by factors C_R and C_X given in Figure 25.

3. For multiple phase wires the value found for one group is divided by the number of wires per phase.

4. For configurations employing flexible-type conduit, use Figures 4 through 17, neglecting the presence of the flexible conduit. This procedure gives results to approximately 10-per-cent accuracy.

5. *Example:* The zero-sequence-impedance of three laced groups of any wire in grounded solid-type conduit at a group spacing of 4 inches and at an elevation above the skin of 4 inches is found from Figure 7, and the curves in Figure 25:

$$Z_0=(0.557)(1.56)+j(1.68)(0.55)$$
$$=0.90+j0.925 \text{ ohms}$$

References

1. IMPEDANCE OF 400-CYCLE THREE-PHASE POWER CIRCUITS ON LARGE AIRCRAFT AND ITS APPLICATION TO FAULT-CURRENT CALCULATIONS, **C. K. Chappuis, L. M. Olmstead.** *AIEE Transactions*, volume 63, 1944, pages 1213–19.

2. PRINCIPLES OF ELECTRIC POWER TRANSMISSION (book), **L. F. Woodruff.** John Wiley and Sons, Inc., New York, N. Y., second edition, 1938.

3. INTRODUCTION TO ELECTRIC POWER SYSTEMS (book), **J. G. Tarboux.** International Textbook Company, Scranton, Pa., 1944.

4. GENERAL ELECTRIC DATA FOLDER NUMBER 63004. General Electric Company, Schenectady, N. Y., January 25, 1943.

5. SYMMETRICAL COMPONENTS (book), **C. F. Wagner, R. D. Evans.** McGraw-Hill Book Company, Inc., New York, N. Y., first edition, 1933.

6. CIRCUIT ANALYSIS OF A-C POWER SYSTEMS (book), **E. Clarke.** John Wiley and Sons, New York, N. Y., volume I, 1943.

No Discussion

Arc Interruption Phenomena in a Magnetic Field at Altitude

J. P. DALLAS
MEMBER AIEE

Synopsis: Arc immobility and arc reversal phenomena limit the use, affect the design, and dictate the test procedure required for aircraft circuit interrupting equipment using magnetic arc suppression. A summary of the literature on this subject is offered. An explanation of the cause of transient arc immobility and small gap arc immobility is proposed. An addition to the consensus of theory as to the cause of arc immobility and arc reversal is suggested usefully relating arc length as a critically important factor to the understanding of these phenomena.

THE aircraft electrical engineer designs to the most rigorous specifications known to the electrical industry and for environmental conditions that would have been regarded as fantastic a few years ago. Extreme conditions of temperature, sand and dust, altitude, vibration, acceleration and humidity, ranging from the environment of the tropical desert sand storm to the stratosphere, are his common problems. While meeting astonishing requirements for the absolute minimum of weight and space he is expected to achieve the absolute maximum of reliability. The aircraft electrical engineer must accomplish these semimiracles because human lives, as well as the completion of military missions on which the safety of the nation may depend, are in turn dependent on the correct functioning of something as "unimportant" as an aircraft switch.

Further to confound the aircraft switch designer, the very laws of physics which earth-bound electrical designers deal with unquestioningly are found to require re-examination. It had been assumed for more than 50 years that an electric arc, like any other conductor free to move in a magnetic field, would move in a direction determined by Ampere's law. This assumption is valid for all practical purposes of circuit breaking equipment operating at sea level, but something happens when Ampere's law is applied to similar equipment at altitude. As the altitude is increased, an electric arc in a magnetic field may falter, stop, and finally reverse its direction of motion.[2,3,9,12,13]

Probably nothing can be more disconcerting to the designer or to those responsible for the testing of equipment than an abrupt discontinuity in characteristics. Pity the poor designer who finds that a switch which will interrupt a large current successfully will not interrupt 10 per cent of that value. That is exactly the type of discontinuous behavior and failure which may be expected with magnetic arc suppression when operated at reduced pressure. This designer's dilemma is illustrated in the curve of Figure 3. A low-travel snap-action switch with magnetic arc suppression is shown to open consistently and stably an inductive 120-volt d-c circuit of 9 amperes from sea level to an altitude of 25,000 feet while failing to interrupt 1 ampere. This disconcerting discontinuity in switch performance was caused by a phenomenon known as "arc immobility" which is a precondition to "arc reversal." It is, of course, ap-

---

Paper 52-333, recommended by the AIEE Air Transportation Committee and approved by the AIEE Committee on Technical Operations for presentation at the AIEE Middle Eastern District Meeting, Toledo, Ohio, October 28–30, 1952. Manuscript submitted August 6, 1952; made available for printing September 9, 1952.

J. P. DALLAS is at 8511 Vicksburg Avenue, Los Angeles, Calif.